Acta Geod Geophys (2017) 52:183–204
DOI 10.1007/s40328-016-0191-3

S.I. : GEOTHERMAL ENERGY SYSTEM

The role of pargasitic amphibole in the formation of major geophysical discontinuities in the shallow upper mantle

István Kovács[1] · László Lenkey[2] · David. H. Green[3] · Tamás Fancsik[1] · György Falus[1] · János Kiss[1] · László Orosz[1] · Jolán Angyal[1] · Zsuzsanna Vikor[1]

Received: 2 June 2016 / Accepted: 30 November 2016 / Published online: 14 February 2017

Abstract Several explanations have been proposed for variation in geophysical properties and depths for the lithosphere–asthenosphere boundary (LAB) and mid-lithospheric discontinuities (MLD). Here, we investigate the proposal that the *dehydration solidus* of pargasitic amphibole-bearing upper mantle with very low bulk water (hundreds ppm) may be one of the main reasons for the observed geophysical anomalies. The *dehydration solidus* may be associated with a very small degree of partial melting in the upper mantle at temperatures and pressures in excess of 1050 °C (for geochemically more depleted) or 1100 °C (for geochemically less depleted upper mantle) and from 1 to 3 GPa (~30 to 90 km) respectively. This small amount of partial melt may be responsible for changes in geophysical properties (e.g. lower seismic velocity, higher attenuation of seismic waves, higher electrical conductivity) in association with the LAB and MLD. This simple petrologic model is tested on the abundant geophysical data of the Carpathian–Pannonian region (CPR), central Europe. The high resolution heat flow data available in the CPR allows us to estimate the depths to intersection of area specific depth-temperature curves with the *dehydration solidus* temperatures (1050 and 1100 °C isotherms). There is relatively small mismatch (<5 km) between the position of these intersections and the geophysically determined LAB in the central area of the CPR. These observations lend support for the proposition that the *dehydration solidus* may be largely responsible for depth variation of the LAB in young continental rift areas. Towards the margins of the CPR, however, where the heat flow is lower ($\lesssim$70 mW/m^2), the predictive capability of the *dehydration solidus* model deteriorates. This is because, for lower geothermal gradients, pargasitic amphibole breaks down at ~90 km (or ~3 GPa) before temperature exceeds the *dehydration solidus* temperatures. Consequently, at ~90 km depth we expect no changes in geophysical properties indicative of hydrous silicate melt, in areas where

✉ István Kovács
kovacs.istvan.janos@mfgi.hu

[1] Geological and Geophysical Institute of Hungary, Stefánia Street 14, Budapest, Hungary

[2] Department of Geophysics, Eötvös University, Pázmány Péter Street 1/C, Budapest 1117, Hungary

[3] University of Tasmania, Hobart, Australia

surface heat flow is lower (i.e. Precambrian cratonic shields, Phanerozoic continental lithospheres or, possibly older oceanic plates). Alternatively, in these areas, the intersection of the geotherm with pargasitic amphibole breakdown may cause small changes in properties which correlate with the MLD rather than the LAB, which is at deeper levels.

Keywords Lithosphere–asthenosphere boundary (LAB) · Mid lithosphere discontinuities (MLD) · Amphibole · Melt · Water

1 Introduction

The lithosphere–asthenosphere boundary (LAB) is one of the most fundamental discontinuities in the Earth's interior separating the outer, rigid lithosphere from the convective and more plastic asthenosphere underneath. The classic view of plate tectonics is that the rigid but fragmented outer shell (lithosphere) floats on the less viscous asthenosphere with relative plate movements driven by ridge push, subduction pull and active asthenospheric flows or the combination of these forces. The LAB is thus a rapid change of viscosity over a small depth interval and such a rheological change cannot be sensed directly by geophysical techniques. However, seismic velocities, seismic attenuation and electrical conductivity can be measured and layers showing generally lower seismic velocity, greater seismic attenuation and higher electrical conductivity are commonly assumed to equate with the asthenosphere. With this simplifying and reasonable assumption, the LAB represents the uppermost part of the global low velocity zone (LVZ) which extends from the LAB to the Lehman boundary at $\sim$220 km depth (Fischer et al. 2010). Yet, more than 100 years from the early theory of continental drift (Wegener 1912; Carey 1958), and more than 50 years after the birth of the modern theory of plate tectonics (Dietz 1961; Wilson 1963; Mason and Raff 1961) there is still no consensus as to what causes the weakening at the LAB and whether the seismological and electrical discontinuities/layers should be equated to the rheological boundaries. In addition, there is still an ongoing controversy how LAB is related to sometimes multiple discontinuities found in cratonic and thicker continental lithospheres (i.e. mid-lithosphere discontinuities referred to as MLD(s) hereafter) (Thybo 2006; Abt et al. 2010; Selway et al. 2015; Karato et al. 2015). As well as rheological, seismological and electro-magnetic properties of the upper mantle, thermal/heat-flow and density/gravity observations must also be reconciled with mineralogical and petrological characteristics of inferred or sampled upper mantle compositions. Heat-flow and inferred geothermal gradients are particularly important in their relationship to melting in the mantle and as sensors for thermal perturbations in plate tectonics (McKenzie 1978; McKenzie and Bickle 1988).

It is not our primary aim here to give a comprehensive overview of processes that have been already invoked to explain the rheological weakening and geophysical properties characteristic for the LAB and MLD. Instead, after a brief discussion of these proposals, we test the application of a petrological model involving the stability of pargasitic amphibole (e.g. Green 1971, 1973; Green and Liebermann 1976; Green 2015) and solidi of lherzolitic mantle, containing very small water (and carbon). For this we will include heat flow, seismic and magnetotelluric (e.g. Horváth 1993; Posgay et al. 1995; Tari et al. 1999; Horváth et al. 2006) data with dense areal coverage from the Carpathian Pannonian region, central Europe (CPR), which is an excellent 'natural laboratory' to test this petrologic model.

2 Theoretical background

2.1 Overview on petrologic models for the LAB based on high pressure experimental study of the mineralogy and melting relations of mantle peridotite

2.1.1 Hydrolitic weakening

Olivine (Mg# ~90) and pyroxenes (orthopyroxene > clinopyroxene) are the dominant minerals stable in the uppermost mantle with lherzolitic compositions and much effort has been applied to determining the physical properties of these minerals as functions of pressure and temperature. Studies have demonstrated the presence of trace water in defect sites in olivine and pyroxenes, which are nominally anhydrous minerals (NAMs, e.g. Smyth et al. 1991; Bell and Rossman 1992). It has been argued that trace water in olivine and pyroxenes as structural hydroxyl in particular sites causes 'hydrolitic weakening' (Kohlstedt et al. 1996; Hirth and Kohlstedt 1996). If the lithosphere has lower water contents because of melt extraction at mid-ocean ridges, the residual depleted peridotite approaches an anhydrous state and thus becomes high strength lherzolite to harzburgite. The inferred higher concentration of 'water' in the undepleted asthenosphere leads to 'hydrolytic weakening' of the mineral structures causing lower seismic velocities and higher seismic attenuation. In addition, the elevated 'water' contents of NAMs contribute to the higher electric conductivity. In this interpretation, the asthenosphere and lithosphere are both subsolidus but differ in water content in olivine and pyroxenes. No significance is attached to pargasitic amphibole stability. In addition a recent experimental study demonstrated that the weakening of mineral structures due to the incorporation of 'water' in NAMs as structural hydroxyl may not be significant (Girard et al. 2013).

2.1.2 Elastically accommodated grain boundary sliding

Elastically accommodated grain boundary sliding (EAGBS for short; e.g. Karato 2014; Karato et al. 2015) has also been proposed as the main mechanism responsible for changes seen in mineral properties at the LAB. This theory implies that, at moderate temperatures, grain boundaries weaken, thus, grain boundary sliding facilitated by elastic deformation of grains can occur. Consequently during the transition from elastic to anelastic behavior with increasing temperatures, there is a point when EAGBS takes place. This produces a temperature and frequency-dependent band in seismic attenuation. The lowering of the elastic modulus results in low seismic velocities of polycrystalline aggregates, such as mantle peridotites. Experimental studies, however, demonstrated that EAGBS may be very sensitive to grain size, 'water' content in NAMs and modal compositions of mantle peridotites. The effects of these factors are poorly constrained, creating uncertainty in P–T conditions under which EAGBS is effective. Calculations involving the currently available experimental data indicate that the temperature at which EAGBS occurs is most probably at ~900 to 1000 °C (Jackson and Faul 2005; Jackson et al. 2014; Karato et al. 2015). This is very similar to the water-saturated solidus of pargasitic amphibole-bearing lherzolite (*water-saturated solidus* is 980–1025 °C from 1.5 to 2.5 GPa, Fig. 1), and also overlaps the solidus for carbonatite melt (930 °C at 2 GPa; Green 2015). Thus, EAGBS can be considered as a potential mechanism for influencing mineral properties at the LAB (or MLDS), but its distinction from the effects of partial melting may be difficult.

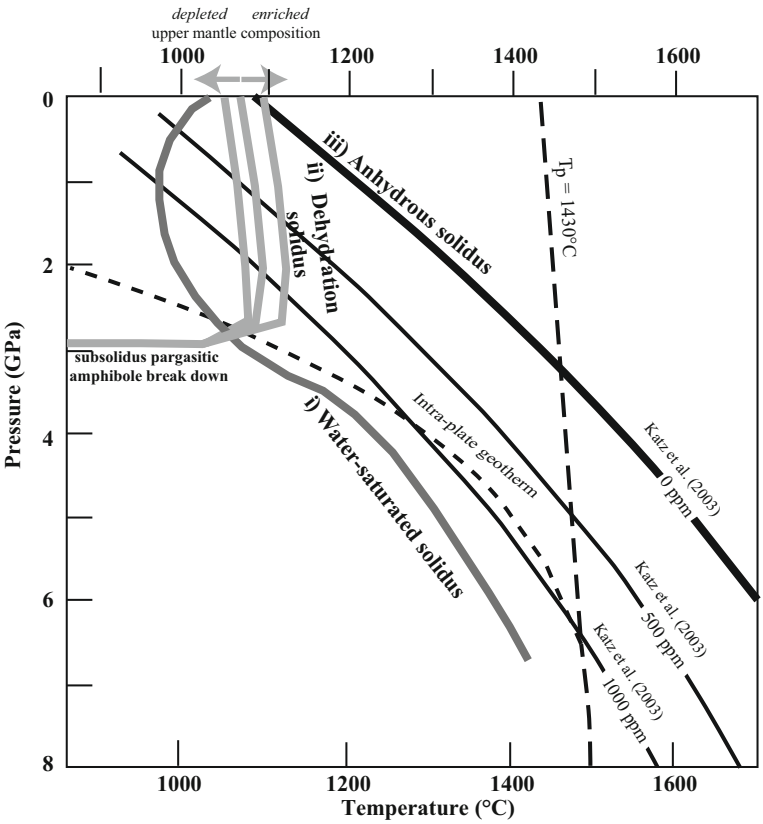

Fig. 1 The positions of the (*i*) 'Water-saturated' (bulk $H_2O \geq 0.4$ wt%); (*ii*) '*Dehydration*' (0.4 wt% $\geq$ bulk $H_2O \geq$ 190 wt% ppm) and (*iii*) 'Anhydrous' solidus (190 wt% ppm $\geq$ bulk H_2O) of upper mantle lherzolite in the P–T space. The Figure is modified after Fig. 3 in Green (2015). Calculated solidus temperatures for various bulk water contents in ppm after Katz et al. (2003) are also *highlighted*. The position of an 'Intra-plate' geotherm was also plotted for a comparison. Different *dehydration solidi* temperatures correspond to upper mantle compositions with different degree of enrichment or depletion (see text for detailed explanation). It is ~1050, 1100 and 1150 °C for refractory (Tinaquillo lherzolite, TLZ), slightly depleted (MORB source mantle, MPY) and enriched (Hawaiian pyrolite, HPY) upper mantle (Wallace and Green 1991)

Besides, the models summarized above several other explanations such as compositional layering and variations in the geometry of seismic anisotropy in the upper mantle may explain the observed seismic anomalies. Selway et al. (2015), however, proposed based on a summary of natural xenoliths that these factors could only act on a local scale and may not explain the global presence of major discontinuities such as the LAB or MLD.

2.1.3 Partial melting and the role of pargasitic amphibole

An alternative to these hypotheses is that the lithosphere is subsolidus but with increasing temperature along the geotherm (i.e. depth-temperature curve), the solidus of mantle peridotite is crossed (and the intersection equates to the LAB) and the asthenosphere has interstitial melt present. The presence of a small amount (maximum ~1 to 2 wt% but

typically significantly less) of partial melt causes the changes in geophysical properties associated with the LAB and MLD. There is a general agreement that a small amount of partial melt could significantly reduce seismic velocities (Kawakatsu et al. 2009; Takei and Holtzman 2009), increase conductivity (Ni et al. 2011) and seismic attenuation (Hammond and Humphreys 2000), but it is debated whether even small degree of partial melting could occur under conditions prevailing in the vicinity of the LAB and MLD (Karato et al. 2015).

Pargasitic amphibole, is found in natural lherzolites, including lithospheric mantle sampled from slow-spreading ridges and fracture zones, and peridotite xenoliths from kimberlites and silica-undersaturated primary basalts (e.g. Griffin et al. 1984; Konzett et al. 2000; Szabó et al. 2004). Pargasitic amphibole contains essential Na_2O and TiO_2 and from 1.5 to 2 wt% H_2O and its stability in lherzolitic compositions is well determined experimentally as a function of pressure, temperature and composition (enriched and depleted lherzolite compositions; Green 1973;Wallace and Green 1991; Niida and Green 1999; Green et al. 2014). In a model mantle (see Green et al. 2014; Green 2015 for details) the pargasitic amphibole composition and modal abundance are controlled by P, T and water content, and pargasitic amphibole may form up to 25 wt% at $\sim$1000 °C and 1–2 GPa (Niida and Green 1999) in slightly depleted compositions (middle ocean ridge pyrolite: MPY, HZ lherzolites) or enriched compositions (Hawaiian pyrolite: HPY). Most importantly, at lithospheric pressures, pargasitic amphibole is stable up to 3 GPa and three distinctive solidi must be considered (Green et al. 2010; Green 2015; see Fig. 1 for an overview):

(i) the *water-saturated solidus* if the water content exceeds that the storage capacity defined by the modal pargasitic amphibole and NAMs ($\gtrsim$0.4 wt%) at pressures <3 GPa., or the storage capacity of NAMs ($\gtrsim$190 ppm) at >3 GPa.

(ii) the *(pargasitic amphibole) dehydration solidus* if water content exceeds that which can be stored in NAMs ($\gtrsim$190 ppm) but is less than the storage capacity defined by the modal pargasitic amphibole and NAMs ($\lesssim$0.4 wt%) at pressures <3 GPa.

(iii) the solidus with bulk water content less than that which can be stored in NAMs ($\lesssim$190 ppm), thus approaching the *anhydrous solidus*.

The important role of pargasitic amphibole in defining the dehydration solidus in the uppermost mantle, despite being crucial, has been generally overlooked or omitted possibly because of: (1) unfamiliarity with the amphibole: pargasitic amphibole and its role in the lherzolite phase equilibria; (2) unawareness on the roles of minor components (i.e. Na, Ti, K) in stabilizing pargasitic amphibole or phlogopite to high temperature at upper mantle conditions; (3) ignorance of the roles which extremely incompatible elements (such as H, K, P, and C) have in introducing additional rare subsolidus minerals and in lowering solidus temperatures (i.e. 'fluxing' melting); (4) unfamiliarity with the role of 'incipient melting' in lherzolite. A very small melt fraction, enriched in volatile and highly incompatible components, is present over a large temperature interval, until temperature approaches the *anhydrous solidus* (Fig. 1) for an upper mantle lacking C–H–O vapour or highly incompatible element-rich phases; (5) paucity of data on the rheological, seismological and electrical conductivity effects of extremely small melt fractions of hydrous silicate melts, including their distribution and porosity/permeability effects.

2.2 The importance of the pargasitic amphibole-based petrological model

In the petrological model adopted here including the role of pargasitic amphibole, the LAB is interpreted as the high pressure or temperature limit of pargasitic amphibole stability so

that the geotherm passed from subsolidus pargasitic amphibole-bearing lherzolite to pargasitic amphibole-free lherzolite with a small melt fraction (<1 wt%; Fig. 1). Consequently, the asthenosphere is a layer with incipient melting, the melt fraction being controlled by the volatile components, particularly H_2O (Lambert and Wyllie 1970; Green 1971, 1973; Green and Liebermann 1976).

It is not surprising that, without taking into account the role of pargasitic amphibole and the *dehydration solidus* (Fig. 1), it has remained challenging to explain the existence of a small melt fraction in the shallow upper mantle at the LAB or MLD. This is because the *anhydrous solidus* temperature of shallow upper mantle peridotite increases almost linearly from ~1100 °C at ambient pressure to ~1420 °C at 3 GPa (Fig. 1). *Anhydrous solidus* temperatures generally exceed, at least by 200 °C, those typical for a normal intra-plate geotherm at a given depth (Fig. 1). Thus, partial melting of anhydrous upper mantle peridotite could not explain the presence of a small amount of partial melt at the LAB or MLD.

Theoretical models on the effect of several hundred to thousands ppm of water in nominally anhydrous minerals (NAMs) in lherzolite (Katz et al. 2003; Hirschmann 2010) predicted decrease of the solidus temperature of mantle peridotite to intersect geotherms as in Fig. 1. These models disregarded the role of pargasitic amphibole. Katz et al. (2003) argued that the presence of 500 and 1000 ppm bulk water reduces the *anhydrous solidus* temperature by ~150 and 200 °C, respectively, at a given pressure (Fig. 1). In this model, one would need at least 1000 ppm water generally in the shallow upper mantle to intersect the intra-plate geotherm at depths characteristic for the LAB or MLD (Fig. 1). Such large amount of bulk water, however, is inconsistent with our present knowledge on the average storage capacity for water in the Earth's upper mantle. Experimental works as well as studies on natural upper mantle peridotites revealed that normal MORB-source upper mantle contains only ~50 to 200 ppm water (Michael 1988; Danyushevsky et al. 2000; Saal et al. 2002; Green et al. 2010; Peslier 2010; Kovács et al. 2012a, b; Warren and Hauri 2014; Demouchy and Bolfan-Casanova 2016; Xu et al. 2016). This is significantly less than what would be needed (~1000 ppm) in the Katz et al. (2003) model to intersect intra plate geotherms and initiate partial melting in the shallow upper mantle (Fig. 1). Only OIB, enriched-MORB and island arc upper mantle sources appear to acquire up to 300–1000 ppm water (Dixon et al. 2002; Hauri et al. 2002; Asimow et al. 2004) but their localized appearance could not explain the global presence of the LAB or MLDs. Intersection of geotherms with the *water saturated solidus* of enriched mantle predicts partial melt at ~75 km in the upper mantle, or at greater depths for cooler geotherms (Fig. 1). At depths $\lesssim$90 km, more than 0.4 wt% bulk water is necessary for water saturation in enriched lherzolite (i.e. exceeding the water storage capacity of pargasitic amphibole lherzolite). Such high water contents may only be present in the immediate vicinity of subduction zones. In intraplate locations it is the *dehydration solidus* which is relevant.

Intersection of model geotherms with the (pargasitic amphibole) *dehydration solidus* predicts partial melt at <90 km only in areas of high heat-flow. The depth of the intersections increases with decreasing heat flow to a 'critical' or 'optimal' heat–flow. This is the expected behaviour of aging oceanic lithosphere at increasing distance from a mid-ocean ridge. It is also the expected behaviour for thermal relaxation from a perturbed geotherm caused by lithospheric thinning, rifting, asthenospheric upwelling, and intraplate basaltic volcanism. The perturbed heat-flow approaches the pre-rifting or steady state value. At the *'critical'* heat flow, the geotherm intersects the solidus at the inflexion from dT/dP ~0 to negative value. In Fig. 2 this 'critical' heat-flow is below 70 mW/m^2, intersecting the solidus in intraplate locations at ~85 km and 1100 °C (for the MORB pyrolite composition). For further decrease in heat-flow to the 'steady-state' geotherm

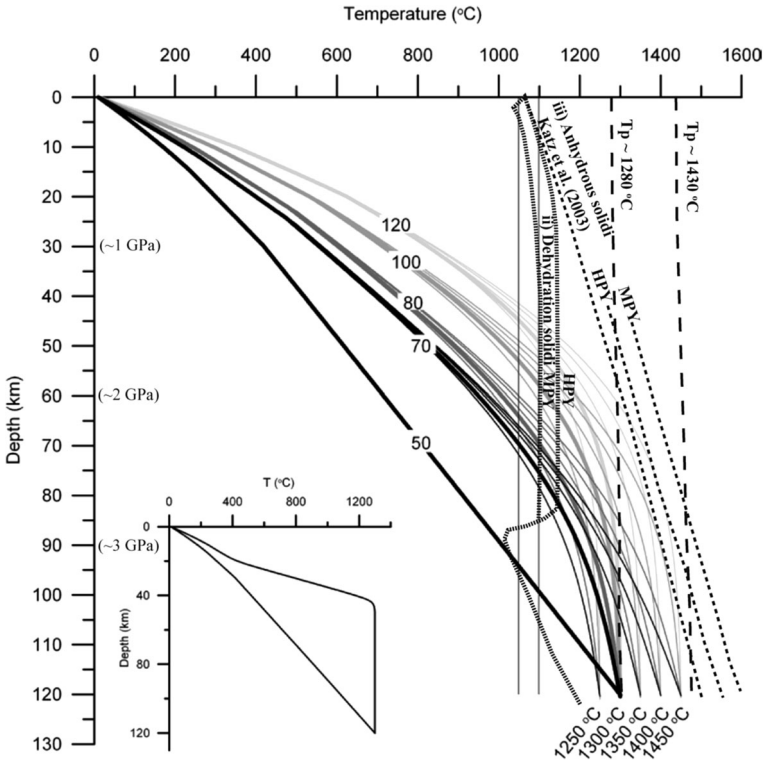

Fig. 2 Geotherms calculated from a non-uniform stretching model (Lenkey 1999 using the model of Royden and Keen 1980), except curve 50, which is a steady-state geotherm. The labels on the curves refer to observed heat flow values (in mW/m^2) in the CPR near to seismic section PGT-1. *Thick curves* are calculated with the usual boundary condition of 1300 °C at 120 km depth (McKenzie 1978; Royden and Keen 1980). *Inset* initial geotherm before stretching and the geotherm just after stretching. Geotherms calculated based on different assumed temperatures (1250, 1350, 1400 and 1450 °C) at 120 km are also indicated (see text for more details). The position of the *dehydration* and *anhydrous* solidi for different bulk upper mantle compositions are also indicated. *Dense dotted lines* indicate the position of the *dehydration solidi* for MPY and HPY (see Fig. 1 for these abbreviations) upper mantle compositions, whereas *less dense dotted lines* shows the position of the *anhydrous* solidi for MPY, HPY and Katz et al. (2003) as well. The *least dotted lines* represent the adiabats for mantle potential temperatures for 1280 and 1430 °C

chosen as 50 mW/m^2, the solidus intersection remains at 80–90 km depth, even though the *dehydration solidus temperature* at this depth drops to 1050 °C (Fig. 2). These depths and temperatures are typical for the LAB in oceanic or young continental lithosphere, or MLDs in sub-cratonic lithosphere.

Our major argument is that the lithospheric and asthenospheric mantles contain H_2O and pargasitic amphibole is a stable phase in the lherzolitic upper mantle at low bulk water contents characteristic for MORB mantle ($\sim$200 ppm) or higher water contents as in OIB or intraplate mantle. Thus, the solidus of the shallow upper mantle is generally the *dehydration solidus* to 90 km depth ($\sim$3 GPa) and *the vapour-saturated solidus for lherzolite (+ C,H,O)* at greater depths. We have used a previously published model for the thermal behaviour of stretched and thinned lithosphere, accompanied by adiabatic asthenospheric upwelling (Royden and Keen 1980). In pressure (depth) and temperature space, by overlaying the experimentally determined solidi for depleted and enriched model mantle

compositions on to the model for lithospheric thinning, we predict a distinctive melting pattern due to the role of pargasitic amphibole in water storage and control of the solidus to ~90 km depth. As previously argued this melting behaviour provides an explanation for the LAB and the upper and lower boundaries of the LVZ. It is also important that the amount of melt generated at the dehydration solidus is dependent on the subsolidus water content (modal pargasitic amphibole) (Green and Liebermann 1976; Green et al. 2014; Green 2015).

3 Methodology

3.1 A possible empirical test of the applicability of the dehydration solidus

The shape of the *dehydration solidus* (Fig. 1) has important implications for predicting the onset of partial melting in the shallow upper mantle which may approximately equate the position of the LAB or MLD:

1) The *dehydration solidus* has roughly constant temperatures [~1050 °C for more depleted compositions (Tinaquillo Lherzolite), and ~1100 °C for less depleted compositions (MOR Pyrolite, HZ lherzolite, Green 2015) in the depth interval between 1 GPa (~30 km)[1] and 2.8 GPa (~84 km; Fig. 1). The *pargasitic amphibole lherzolite dehydration solidus* temperature is slightly higher (~1150 °C) for even more enriched compositions (Hawaiian Pyrolite, NHD peridotite; Wallace and Green 1991; Green 2015), however, we use the lower temperatures (1050 and 1100 °C) corresponding to depleted peridotite as it resembles more closely the composition of the upper mantle beneath the CPR (see our following chapter on xenoliths). The term 'depleted' means that the upper mantle is depleted in volatiles (e.g. C, H) and incompatible elements (e.g. Al, Ca, Fe, Na, K). This means that in this depth interval the presence of partial melt is expected if the geotherm reaches the *dehydration solidus* temperatures. Geotherms in Fig. 2 specific for the CPR (see how these were derived in following chapter) refer to the depth-temperature curves for specific surface heat flow values whereas the 1050 and 1100 °C isotherms approximate to the *dehydration solidi* between 1 and 2.8 GPa.

2) There is a sharp *negative* dT/dP in the dehydration solidi between 2.8 and 3 GPa (Fig. 1), with the solidus temperature *decreasing* by 50–100 °C with increasing pressure over a depth interval of 5–6 km (e.g. Green 1973; Niida and Green 1999; Green and Falloon 2005; Green et al. 2014; Green 2015). This means that the depths of intersections of geotherms calculated for heat flows of ~slightly below 70 mW/m^2 with the solidus for lherzolite with ~200 ppm water remain stable at ~85 to 90 km depth. Equally, for the early stages of a developing continental rift, upwelling asthenosphere freezes to pargasitic amphibole (±phlogopite) lherzolite at 85–90 km depth (Figs. 1, 2) until the temperature at this depth exceeds the *dehydration solidus temperatures*. If the uppermost part of the asthenosphere in intraplate regions is depleted lherzolite then the LAB does not move to shallower depths (thinning of lithosphere) until the heat flow exceeds ~70 mW/m^2. If the geotherm exceeds that calculated for ~70 mW/m^2, then the intersection with the *dehydration solidus* moves rapidly to shallower depths. This heat flow is the already defined *critical heat flow* which may be different in other tectonic setting, depending on the area specific depth-temperature curves. The use of the *dehydration solidus* to map the depth of

[1] For the calculation, we generally assumed ~3 g/cm^3 density for the lithosphere where 1 Kbar or 0.1 GPa correspond to ~3 km thickness.

the LAB in an intraplate setting of stretching and rising geotherms predicts an initial slow heating with no change to the lithosphere thickness followed by a sharp change to more rapid rifting, rise of the LAB and increasing intraplate magmatism.

In this paper, we attempt to test the predictions of the *dehydration solidus* for the LAB in the CPR using geophysical data. First it is assessed whether the depths of the 1050 and 1100 °C isotherms (approximating to the *dehydration solidi* at 1–2.8 GPa or ~30 to 85 km) in the Pannonian Basin (referred to PB hereafter) coincide with the location of the geophysically constrained depth of the LAB. This is because the PB is a young continental rift in the central CPR with highly attenuated lithosphere and high surface heat flow ($\gtrsim$70 mW/m^2) generally exceeding the *critical heat flow* where depth-temperature curves are expected to cross the *dehydration solidus* depths <85–90 km (see preceding discussion; Fig. 1). The PB is an excellent natural laboratory for such test as numerous surface heat flow data, specific depth-temperature curves (geotherms), joint seismic and magnetotelluric constraints on the depth of the LAB are available (Lenkey 1999; Lenkey et al. 2002; Horváth 1993; Tari et al. 1999; Horváth et al. 2006, 2015). Our approach is somewhat simplified in the sense that the shape of the *dehydration solidus* is approximated by constant (1050 and 1100 °C) temperatures between 1 and 3 GPa to simplify calculations. As the Moho discontinuity is at ~25 to 30 km depth beneath the PB the small positive dT/dP at <1 GPa is not considered. On the other hand, the strongly negative dT/dP at 2.8–3 GPa effectively fixes the LAB at 85–90 km as previously discussed. By ignoring any curvature in the solidus between 2.5 and 3 GPa our results may overestimate the depth of the LAB only by a few km in this range.

3.2 Determination of temperature-depth curves and the depth of the 1050 and 1100 °C isotherms for the PB

The PB was formed by lithospheric extension during the Middle Miocene (Royden et al. 1983; Csontos et al. 1992; Horváth 1993) and this was accompanied by asthenospheric uplift resulting in high surface heat flow (Dövényi and Horváth 1988; Lenkey et al. 2002). Since the formation of the basin, the lithosphere has been cooling as evidenced by thermal subsidence and accumulation of thick Neogene and Quaternary sediment pile (Magyar et al. 2012). Therefore, steady state thermal models similar to those applied to the Fennoscandinavian Shield (Artemieva 2009) or the Canadian Shield (Jaupart et al. 1998) cannot be applied to estimate the geotherm in the lithosphere. We used the non-uniform stretching model of Royden and Keen (1980), which takes into account the transient cooling of the lithosphere, and allows the different amounts of stretching of the crust and lithospheric mantle. Additionally, we took into account the radioactive heat production in the upper crust. The inset in Fig. 2 shows the initial geotherm before stretching and just after stretching. Following the stretching, the lithosphere cools and the temperature returns to its initial value, which takes about 100 million years. Given the stretching factors of the crust and the lithospheric mantle the model predicts the evolution of the surface subsidence and heat flow.

The crustal and lithospheric mantle stretching factors for the model were derived in 5 × 5 km grid in the PB by equating the model-predicted present day heat flow and the total accumulated sediment thickness with the observed values (Lenkey 1999). The thermal parameters of the model are given in Table 1. It is evident that, in case of higher heat flow, the stretching factors are also higher, and the geotherm in the lithosphere is steeper. We choose four places near to the Pannon Geotraverz-1 (PGT-1) seismic section where the heat flow is 70, 80, 100 and 120 mW/m^2, respectively, and using the stretching factors

Table 1 Parameters and their respective references applied for the calculation of depth-temperature curves

Parameter	Value
Initial crustal thickness[a]	35 km
Initial lithospheric thickness[a]	120 km
Density of crust[a]	2800 kg/m^3
Density of mantle[a]	3300 kg/m^3
Temperature at the surface[a]	10 °C
Temperature at 120 km depth[a]	1300 °C
Thermal expansion coefficient[a]	3.1×10^{-5} l/°C
Thermal diffusivity[a]	7.8×10^{-7} m^2/s
Heat production in the upper crust[b]	8×10^{-7} W/m^3
Thickness of the upper crust[c]	15 km

[a] McKenzie (1978)

[b] Jaupart and Mareschal (1999)

[c] Posgay et al. (1995); Hajnal et al. (1996)

previously derived (Lenkey 1999) and belonging to these locations, the present day geotherms were calculated (thick lines in Fig. 2) and the intersections of the geotherms with the *dehydration solidus* temperatures (1050 and 1100 °C) were determined.

In their influential paper on the thermal behaviour of crustal stretching and consequential mantle upwelling, McKenzie and Bickle (1988) divided the Earth's upper mantle into underlying convecting layer, assumed to have an adiabatic temperature gradient, overlain by a thermal boundary layer in which the gradient is steeper (super-adiabatic) from surface temperatures to intersect the mantle adiabat at depths determined by local heat flow and thermal conductivity. The term 'mechanical boundary layer' (MBL) referred to the uppermost mantle and crust with conductive heat transfer, overlying a transitional layer ('thermal boundary layer') (TBL), also with dT/dP greater than the adiabatic geothermal gradient.

In our thermal model the bottom of the thermal lithosphere is at 120 km depth and 1300 °C based on the analysis of the ocean floor bathymetry (McKenzie 1978 after Parsons and Sclater 1977). This depth and temperature for the base of the thermal lithosphere, however, seems to be inconsistent with petrological models at the first sight (cf. Green 2015). This discrepancy arises from different uses of 'lithosphere' as we discussed above. The geophysical model uses the thickness of the thermal lithosphere and not the petrological or rheological lithosphere (e.g. Artemieva 2009). By definition from thermal point of view, we can distinguish the conductive, transitional and convective part of the upper mantle. The conductive (MBL) part can be equated to the petrological lithosphere. The thermal lithosphere, however is thicker and has a transitional thickness between the purely conductive and convective upper mantle (TBL) (Artemieva 2009). It follows that the thermal lithosphere includes the upper part of the asthenosphere as well. Consequently the 1300 °C at 120 km is consistent with the petrological model, since 120 km is not the thickness of the petrological lithosphere but that of the thermal lithosphere. The temperature at the top of the purely convective asthenosphere is referred to as the potential temperature (T_p) and is assumed to be ~1430 °C for the modern Earth (Green 2015). At the bottom of the thermal lithosphere the temperature approaches T_p, which we assumed to be 1300 °C but its value is uncertain. Uncertainty in this temperature is explored by varying its value from 1250 to 1450 °C. Therefore, geotherms corresponding to heat flow of 50 to 120 mW/m^2 are calculated to intersect a range of adiabatic gradients at a chosen depth of 120 km, and temperatures of 1250–1450 °C (i.e. corresponding to Tp ~ 1210–1410 °C). The geothermal model is quite robust, because the depth to the

intersections with 1050 and 1100 °C isotherms differ between 3 km (1250 °C) to 5 km (1450 °C) (Fig. 2). This means that the solidus/geotherm intersections lie at slightly shallower depth if the assumed temperature at 120 km depth is higher and vice versa. The inset Fig. 2 illustrates a steady-state or pre-thinning geotherm for 50 mW/m^2 perturbed instantaneously by asthenospheric upwelling with Tp $\sim$ 1300 °C.

4 Results and discussion

4.1 The depth of the 1050 and 1100 °C isotherms beneath the CPR and implications

Using the geotherms calculated from the stretching model the local positions to the *dehydration solidus* temperatures (1050 and 1100 °C) in the CPR were mapped (Fig. 3a, b). The maps reveal that the geotherm intersections with 1050 and 1100 °C isotherms are shallower than 90 km in the PB, which is characterized by heat flow values exceeding the critical value ($\gtrsim$70 mW/m^2). The depth of both geotherm/solidus intersections decreases rapidly from below 90 km at the boundaries of the CPR to $\sim$60 km in the inner part of PB. This steepening of the geotherm happens usually over a short ($\sim$100 km) horizontal distance. The depth of the geotherm/solidus intersections (approximated to 1050–1100 °C isotherms) is $\sim$60 km in large part of the central part of the CPR (Fig. 3a, b). Our methodology could not be applied directly to the Transylvanian Basin which has distinct extensional history to the central part of the PB (see also below). There are some locations (Transdanubian Central Range, Mecsek and Bükk Mts.), however, where the geotherm/-solidus intersections are in a deeper position. This deviation is due to the intensive cooling effect of karst water circulation in the Mesozoic carbonate formations in these regions. For the Transdanubian Central range, the relatively lower heat flow can also be related to the relatively thicker MOHO beneath the area ($\sim$30 to 35 km; Kiss et al. 2016).

The difference between the depths of the 1050 and 1100 °C geotherm/solidus intersections are usually within $\sim$6 km under the entire CPR. This is probably in the order of or less than the uncertainty how accurately the depth of the isotherms could be constrained. This difference could represent the apparent variation which arises from geochemistry of pargasitic amphibole as in less depleted mantle sources pargasitic amphibole breaks down at 1100 °C, while those from a more depleted source at only 1050 °C. This means that the pargasitic amphibole break-down in areas with less depleted upper mantle is expected to take place a few kilometers deeper.

Figure 4a, b display the difference in kilometres between the intersection of the local geotherm with the *dehydration solidus* temperatures (approximately at the 1050 and 1100 °C) isotherms and the LAB determined by integrated seismological observations and magnetotelluric soundings. For the overwhelming portion of the PB the difference between the two independently determined LAB depth is less than $\pm$10 km. Consequently, we can state that these results at least do not disagree with the prediction of our simple petrologic model based on the *dehydration solidus*. In fact, the agreement between the position of the intersection of local geotherm and the *dehydration solidus*, and the geophyscially determined LAB is almost within model uncertainty ($\pm\sim$5 km). This reasonable agreement implies that, in areas with similarly high heat flow to the PB (young rift areas and oceanic plates), the position of the *dehydration solidus* (1050 and 1100 °C) may give good first order estimation for the depth of the LAB.

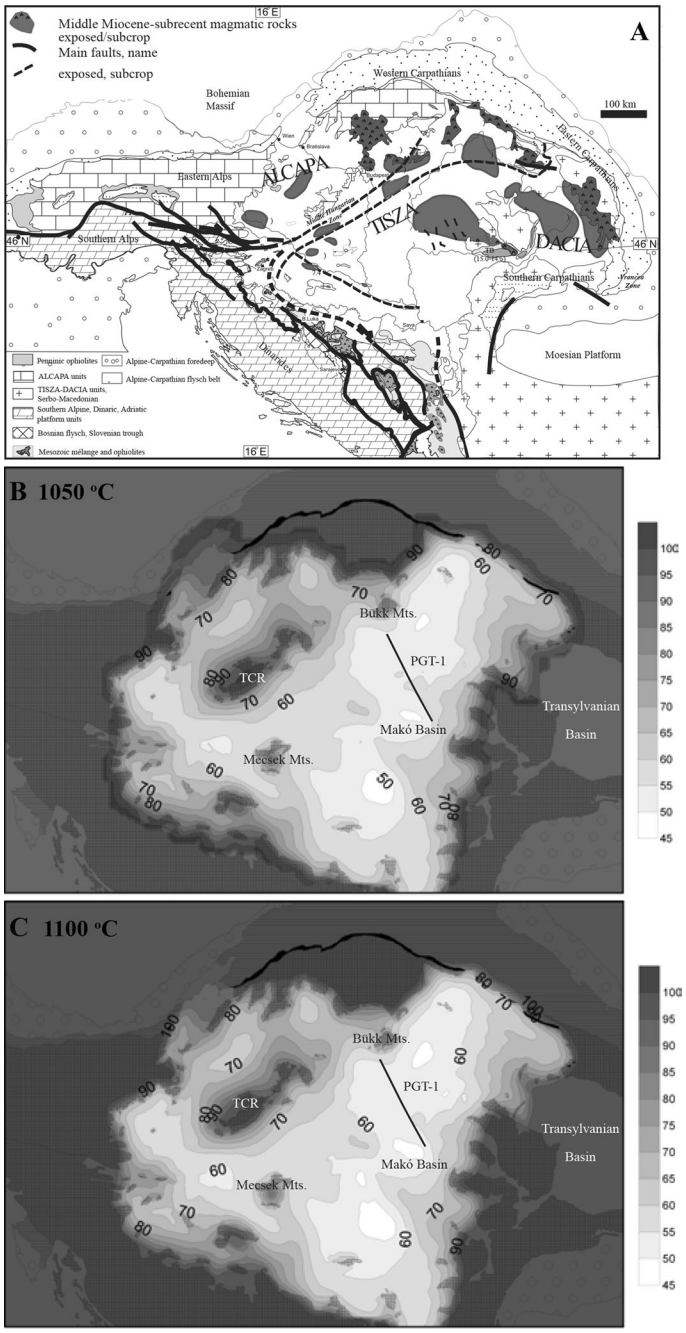

Fig. 3 **a** Schematic geological map of the central Carpathian–Pannonian region (CPR). Major localities are discussed in the text are indicated. Calculated depths of intersection of local geotherm with the *dehydration solidus* isotherms of 1050 °C (**b**) and 1100 °C (**c**) are highlighted beneath the CPR using surface heat flow data of Lenkey et al. (2002) and depth-temperature curves in Fig. 2. The location of the Pannon Geotraverz (PGT-1) geophysical traverse is indicated by a *solid line*

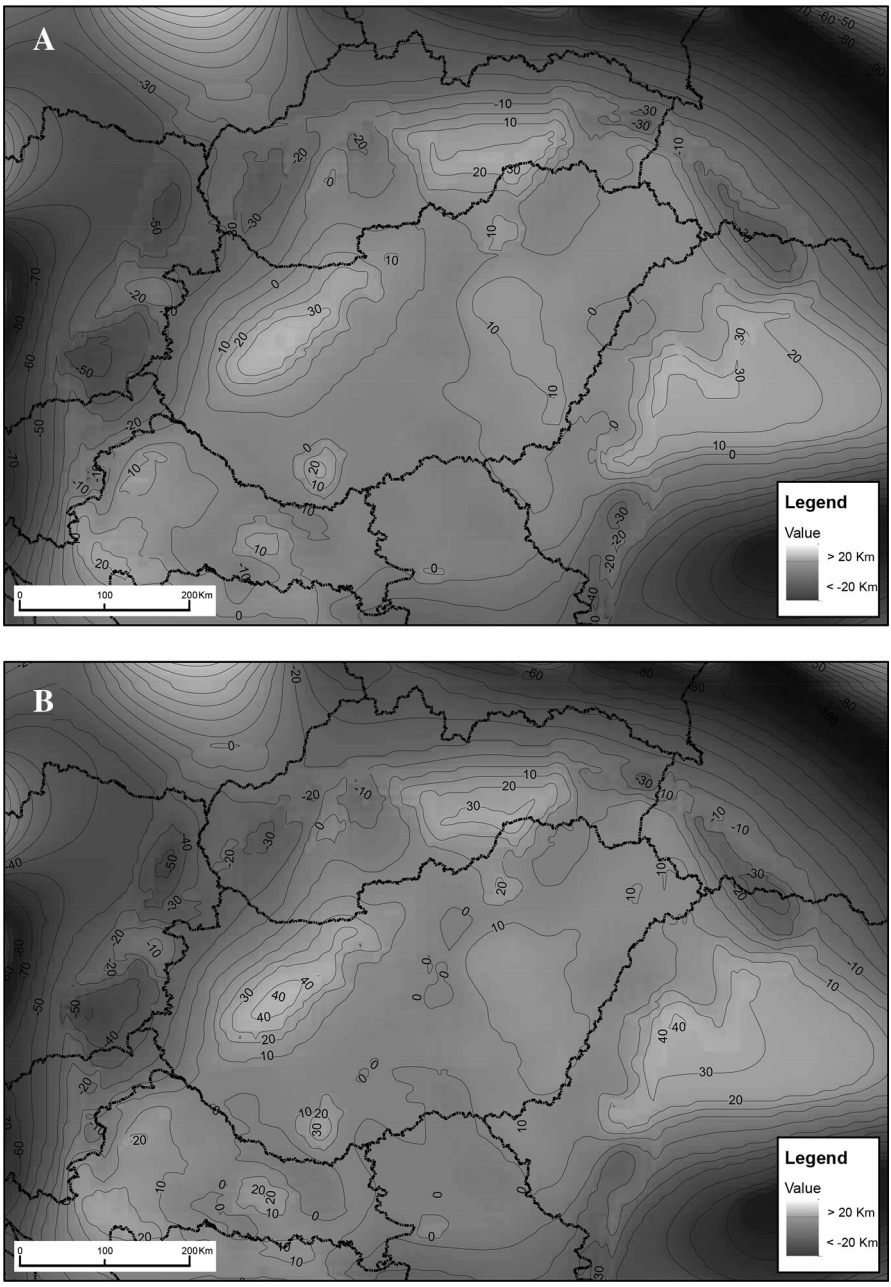

Fig. 4 Difference between the depths of the *dehydration solidus* temperatures 1050 °C (**a**) and 1100 °C (**b**) and the geophysically constrained LAB (Tari et al. 1999) in kilometres

Larger discrepancies exceeding 20 km, in the PB, are usually only observed for areas where surface heat flow is underestimated (due to the presence of carbonate formations, see Fig. 3). At these areas, the position of the *dehydration solidus* isotherms (1050 and

1100 °C) is deeper than the geophysically constrained LAB. The calculated *dehydration solidus* isotherms also predict deeper LAB than the geophysically determined one in the central part of the PB and in the Transylvanian basin (see Fig. 4a, b).

The particular part of the Pannonian Basin, where the calculated dehydration solidus temperatures run deeper than the LAB, is characterized by extremely thinned lithosphere, where the lithospheric thickness is only ~40 km in the Békés basin (at the SE corner of this anomaly). This is also an area where deep basins (e.g. Makó basin and Békés Basin) separated by elevated basement highs (e.g. Battonya high) with a NW–SE strike. These deep basins were formed in the Late Miocene–Early Pliocene (~5 Ma, Early Pannonian; Horváth et al. 2015), after the main phase of larger-scale extension in the CPR (Huismans et al. 2001) in the Middle Miocene. This process may have been associated with the additional localized thinning of the lithosphere which can account for the extremely thin lithosphere in this area. Note that anomalous MOHO was identified in the Békés Basin which may have been the result of basaltic underplating in association with this relatively young regional rifting (Hajnal et al. 1996). The relatively young rifting event here may imply that in this area the thermal equilibrium might not have been completely achieved yet.

The Transylvanian Basin, on the other hand, is an elevated basin (~300 to 400 m above the sea level) between the Apuseni Mts. and East Carpathians, which is characterized by thicker lithosphere and lower surface heat flow than the PB. The discrepancy between our prediction and the observed lithospheric thickness is related to the distinct geodynamic history of Transylvanian Basin, because it was formed by different mechanisms to the PB of which exact kinematics is yet to be revealed (e.g. Krézsek and Bally 2006).

4.2 Xenoliths

It is logical to evaluate whether equilibrium temperatures recorded by upper mantle xenoliths from the central PB (Bakony-Balaton Highland) fit into our thermal approach. The studied xenoliths from the PB span a considerable range of equilibrium temperatures from ~850 to 1175 °C (i.e. Embey-Isztin et al. 1989, 2001; Szabó et al. 2004; Dobosi et al. 2010; Kovács et al. 2012a, b; Embey-Isztin et al. 2014). The mantle xenoliths mainly originate from the lithospheric mantle and only subordinately from the asthenosphere due to the less plastic nature of the former. Thus, the maximum equilibrium temperatures (1175 ± 30 °C) seem to just slightly exceed what we would expect if the LAB was related to the break-down of pargasitic amphibole (i.e. max. 1150 °C in enriched peridotite). This slight discrepancy may be accounted for by the fact that xenoliths record older temperatures of the upper mantle than those estimated from the present day surface heat flow. The age of the alkaline basaltic activity which brought up the xenoliths to the surface is ~5 Ma. It means that there was time for further thermal relaxation involving further subsidence of isotherms. During this process, the upper mantle, which had originally ~1175 °C equilibrium temperature at 5 Ma, cooled at least below the *dehydration solidus* temperature (~1100 °C), presumably. The higher temperatures of some upper mantle xenoliths may also reflect their asthenospheric origin. In either case, the equilibrium temperatures of upper mantle xenoliths from the Bakony-Balaton Highland seem to be in line with our assumption that the LAB can be equated with the *dehydration solidus* temperatures (1050 and 1100 °C) in a young rift area with high heat flow values exceeding the *critical heat flow* ($\gtrsim$70 mW/m^2). In addition, pargasitic amphibole can be found either rarely as a rock-forming mineral constituent or more often in traces in these upper mantle xenoliths (Embey-Isztin 1976; Szabó et al. 2004; Dobosi et al. 2010).

4.3 Implications for the depth of the LAB beneath (young) oceanic plates

In summary, we can state that, albeit our estimation bears uncertainties ($\sim\pm5$ km), the calculated and independently constrained depth of the LAB appears to agree reasonably well (mostly within ±5 km) beneath the PB, where the surface heat flow exceeds the *critical heat flow*. This is the particular heat flow value at which the corresponding geotherm reaches the *dehydration solidus* temperatures (1050 and 1100 °C) shallower than ~3 GPa (~85 to 90 km).

Below with a brief overview of the literature, we explore whether the *dehydration solidus* could predict the depth of the LAB under young oceanic plates where the heat flow is usually above the critical value. Note that Green and Liebermann (1976) already put forward that the top of the low velocity zone (i.e. LAB) under oceanic lithospheres is defined by the intersection of the oceanic geotherm with the *dehydration solidus* of lherzolite from 0.5 to 2.8 GPa at ~1050 to 1100 °C. Because the geotherms become less steep with increasing distance from the mid-ocean ridge, the lithosphere thickens with age and distance from the middle ocean ridge. The steep negative dT/dP of the dehydration solidus at 2.8–3 GPa means that the lithosphere reaches a stable thickness of ~85 to 95 km for oceanic plates older than 80 Ma. Thus it will be evaluated further whether this classic model and in particular the position of the *dehydration solidus* could, indeed, coincide with the depth of the LAB beneath young oceanic plates.

Rychert and Shearer (2011) studied the shape of stacked SS waveforms (SS lithospheric profiling) in the Pacific Ocean and arrived to the conclusion that the depth of the LAB beneath oceanic plates varies from 25 to 130 km and correlates with the distance from the trench. They found that the depth of the detected geophysical anomalies agrees well with the 930 ± 90 °C isotherm(s) calculated from a half-space cooling model with upper mantle potential temperature of 1350 °C and plate velocity of 60 mm/yr. The authors proposed that this boundary should be a permeability boundary with a small amount of melt below it. Note that the proposed 930 ± 90 °C is not very far from the *dehydration solidus* temperatures, especially if we consider that the *dehydration solidus* should be at lower temperatures (~1050 °C) in a depleted oceanic upper mantle. In addition the authors used 1350 °C potential temperature which is considerably lower than the petrologically more reasonable 1430 °C (Green 2015). If the initial starting temperature in their half-space cooling model was higher it is possible that the best fit isotherm would be even closer to the *dehydration solidus* temperature.

Schmerr (2012) stacked a large dataset of SS precursors from oceanic areas and found a sharp velocity contrast at 40–70 km depth. It was found that the depth of the discontinuity show relatively good agreement with the depth of the 900 and 1100 °C isotherms predicted from the half-space cooling model and the plate model respectively. The author attributed this anomaly to the combination of the presence of small amounts of partial melts (0.1–3%) at the base of the oceanic lithosphere, compositional contrast (i.e. depleted asthenosphere below a re-hydrated more enriched lithosphere which had been metasomatised by upward migrating asthenospheric melts) and the cooling of the oceanic lithosphere with age. Localized small-scale convections and hydrations enrichments (i.e. subductions) may further complicate this picture locally. Again, the proposed temperature range overlaps with that of the *dehydration solidus* temperatures. The agreement may be even better if we consider that the author assumed the same low upper mantle potential temperature as Rychert and Shearer (2011) did.

Naif et al. (2013) reported that there is presumably a melt rich layer beneath the oceanic plate subducting below Nicaragua based on electromagnetic soundings. The authors found that the high conductivity zone is between 45 and 70 km, of which upper part at 45 km could be defined as the LAB in our sense. This depth according to the authors is very close to the intersection of a 23 Ma old oceanic geotherm (corresponding to 1420 °C mantle potential temperature) and the solidus of peridotite containing 275 ± 85 ppm 'water'. Alternatively the intersection of an oceanic geotherm (corresponding to 1315 °C upper mantle potential temperature) and a peridotite solidus with 505 ± 155 ppm water would be also at ~45 km. The MORB mantle, however, contains usually 50–200 ppm water which would be insufficient to produce partial melting. Naif et al. (2013) argued that this discrepancy may be explained by the uncertainties in the estimation of the solidus temperature and the presence of other volatiles. We suggest that the stability of pargasitic amphibole at low bulk water contents typical for MORB and the lower temperature of the *dehydration* solidus may more suitably explain this 'discrepancy'. The *dehydration solidus* temperature (1050 and 1100 °C) would intersect their geotherm very close to the expected ~45 km depth.

In summary, it seems that the *dehydration solidus* and the classic petrological model of Green and Liebermann (1976) seem to give a reasonable explanation for the presence of a small amount of partial melts where geophysical anomalies likely indicate the LAB. It should be evaluated further, however, how other volatiles (especially CO_2) and the higher modal abundance of pargasitic amphibole below the dehydration solidus would improve the correspondence between petrological and geophysical constraints on the depth of the LAB beneath oceanic basins.

4.4 Reconciling the relation of the LAB and MLD?

In the marginal areas of the CPR surrounding the PB, where the heat flow is below the *critical heat flow* for the area ($\lesssim$70 mW/m^2) the discrepancy between the *dehydration solidus* temperatures and the geophysically determined LAB becomes large. This makes sense since the pargasitic amphibole breaks down at ~90 km depth uniformly in such areas. In these areas we expect to see a horizon of geophysical anomalies at ~90 km depth. These areas may include older (Phanerozoic) continental and oceanic plates and cratons where surface heat flow is below the *critical heat flow*.

In Fig. 5 it is illustrated how the relation of the LAB and MLD may vary in (1) young continental rifts and oceanic plates, (2) Phanerosoic continental lithospheres and older oceanic plates and (3) cratons. The main point is that in young continental rifts and oceanic basins the identification of the LAB is usually straightforward. In these areas the LAB is mainly related to the break-down of pargasitic amphibole at the *dehydration solidus* temperatures (1050 and 1100 °C isotherms).

In contrast in older Phanerozoic continental lithospheres, older oceanic plates or cratons where the heat flow is below the *critical value,* the pargasitic amphibole breaks down at ~90 km, which should cause geophysical anomalies at a relatively constant depth globally. Thybo and Perchuc (1997) and Thybo (2006) were among the first to reveal the presence of a global layer of geophysical anomalies at ~100 km, referred to as the 8° discontinuity. Its origin, have been explained by several possible scenarios including the presence of partial melt but no significance was attached to the role of pargasitic amphibole. Kind et al. (2012) reported that the top of the LVZ is sharper and appears to be a global horizon (at depth ~100 km). This anomaly seems to be present below cratonic areas as well. Their study was based on receiver function analysis of a global dataset of

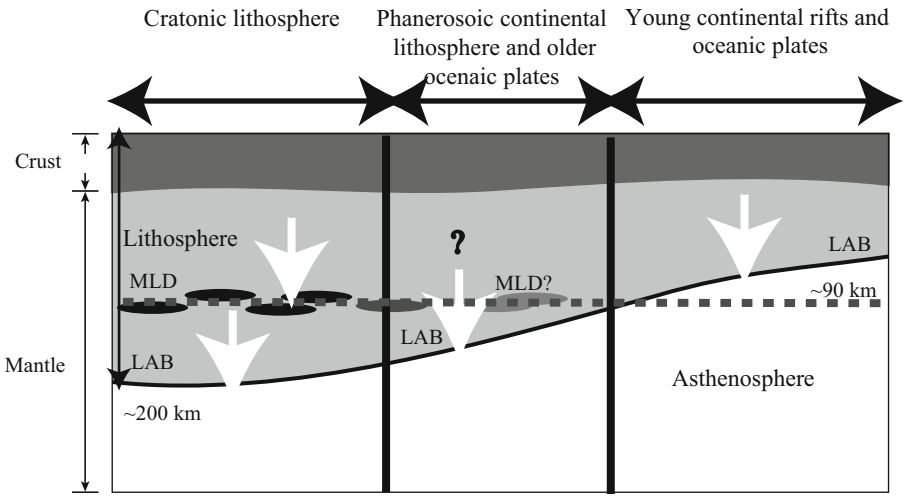

Fig. 5 Variations in the respective positions of the lithosphere–asthenosphere boundary (LAB) and middle lithospheric discontinuities (MLDs) in different tectonic settings. This figure is substantially modified and completed after Fig. 1 in Fischer et al. (2010)

converted S and P phases. Kind et al. (2012) argued that the global anomaly may be related to the role of aluminous orthopyroxene (Mierdel et al. 2007) or EAGBS (Karato 2014). Fischer et al. (2010) also reported a global layer at ~100 km (including oceans and cratons) which is perturbed by upwelling (plumes) and down welling (subductions) in the mantle. This boundary is characterized by steep velocity gradients reflected in ScS reverberations (i.e. a seismic shear (S) body wave that reflects off the core-mantle boundary) and P and S receiver function analysis. They argued that its origin is not only related to the thermal gradient but hydration, presence of melt and anisotropy may all play a role. The ~100 km depth of global geophysical anomalies agrees very well with the upper stability (~90 km) of pargasitic amphibole in areas where heat flow is low. Thus, it appears to be reasonable to attribute the origin of this global boundary layer to the instability of pargasitic amphibole in the upper mantle at low bulk water contents and higher pressures.

Consequently in Phanerosoic continental lithospheres and older oceanic plates, the geophysical anomalies generated by the instability of pargasitic amphibole at 90 km may not always be clearly distinguished from those of the sometimes only slightly deeper LAB (Fig. 5). We argue that in many previous studies the shallower anomalies interpreted as the MLD may be produced by the instaility of pargasitic amphibole at ~90 km (e.g. Abt et al. 2010; Selway et al. 2015). In cratonic areas where the LAB is very deep (>150 km), the anomaly caused by the pargasitic amphibole dehydration can easily be discerned from the LAB by the shallower depth of the former (Fig. 5). This is not to say that all MLDs can be explained in Phanerosoic continental lithospheres, older oceanic plates and cratons by the instability of pargasitic amphibole at ~90 km. What we want to stress here is that some MLDs detected in these areas could be related to pargasitic amphibole dehydration as argued by Selway et al. (2015).

Note that there are similar anomalies present at ~100 km depth in other continental areas with thicker lithosphere as well (e.g. North America, Abt et al. 2010) which are also interpreted as MLDs. Rader et al. (2015) argued that the MLD is the geophysical

manifestation of a geochemical boundary which may be due to the prior intersection of the volatile-rich solidus with cooling geotherms. They also suggested that the MLD marks the former position of the LAB when the lithosphere was tectonically younger and presumably warmer. Rader et al. (2015) implied that the presence of higher modal abundance of phlogopite, carbonate or pyroxene may account for the slower seismic waves at the MLD but attributed only moderate role to the *dehydration solidus*. In their study, the average of accurate geophyscial MLD determinations was ~90 km with the vast majority of the data vary between 80 and 110 km. This agrees very well with the instability of pargasitic amphibole at ~3 GPa (90 km).

In Hansen et al. (2015), the depth of the MLD and LAB was estimated based on S_p receiver function imaging focusing on the position of negative velocity gradients (NVG). The authors proposed that NVGs in the western US indicates the LAB which is at 60–85 km with temperatures between 1200 and 1400 °C. In contrast, the NVGs under the central US and Rocky Mountains are between 70 and 110 km at temperatures 700–900 °C. These are mainly interpreted as MLDs but there is an area between the Rocky Mountains and the central US where the interpretation of NVGs is ambiguous (they could indicate both LAB and MLD). The temperatures were estimated from surface wave tomography model originating from the USArray dispersion measurements using the olivine inelasticity model of Jackson and Faul (2010) assuming an average grain size of 1 mm for upper mantle rocks (this average size appears to be just too large for typical upper mantle peridotites if porphyroclasts are not considered). The model, however, is strongly grain size dependent and larger average grain size could result in higher temperatures. Considering normal intra-plate geotherms (Fig. 2) the MLD temperatures seems to be unusually low while LAB temperatures exceptionally high from petrological point of view. Thus, our preferred interpretation is that in the western US the heat flow should be above the critical value and the dehydration solidus temperatures are reached shallower than ~90 km. Consequently, NVGs under the western US indicate the LAB, however, the corresponding temperatures at that depth should not exceed ~1100 °C, which is much lower what the authors claimed. In the other areas on the east, the heat flow should be below the critical value and pargasitic amphibole breaks down at ~90 km. In our interpretation, the transitional area between the western and central US, where the assignment of the NVGs is ambiguous, represents a situation where it cannot be accurately predicted whether the pargasitic amphibole break-down at ~90 km could correspond to the LAB or MLDs. Further to the east under the central US, the LAB is deeper and can be well resolved from the pargasitic amphibole break down at ~90 km. This depth seems to be in line with the 84 km peak in NVGs' depth under the central US. The calculated temperature (~770 °C) for the MLD, however, appears to be underestimated.

Selway et al. (2015) suggested that MLD phase could be commonly explained by the stability of (pargasitic) amphibole, however, the amphibole alone may not be the universal explanation. The authors argue that in some localities (e.g. Kaapval craton) where the MLD is well constrained and upper mantle xenoliths are available the amphibole is not present in sufficient modal abundance from MLD depths to account for the observed decrease in seismic velocities. Selway et al. (2015) considered only the effect of modal amphibole on seismic velocities but did not take into account the role of small amount of melts/fluids and trace amount of pargasite which should exist at the *dehydration solidus*. It may well be that the combined effect of (very) small amount of modal pargasitic amphibole and underlying incipient melt bearing upper mantle mineralogy may give better fit to their observations. We agree, that the stability of (pargasitic) amphibole is not the only factor in controlling the formation of geophysical anomalies in the upper mantle,

therefore, 'discrepancies' may be reconciled with the consideration of these other factors (e.g. EAGBS, hydrolytic weakening).

5 Conclusions

A simple petrologic model based on the *dehydration solidus* in the shallow upper mantle has been tested whether it is suitable to explain the presence of geophysical anomalies at LAB and MLD depths. In young continental rifts and oceanic plates, where the heat flow is above a *critical value,* the model suggests that the position of the *dehydration solidus* temperatures in the upper mantle (1050 and 1100 °C isotherms) should agree well with the geophysically constrained LAB. In this study, we demonstrated that in the *Pannonian Basin*, which is a young rift area, the depth of these isotherms indeed resemble well with the independently determined depth of the LAB. The critical surface heat flow is the heat flow value at which the area specific depth-temperature curves reaches the *dehydration solidus* temperatures in shallower depth than 3 GPa ($\sim$90 km). This $\sim$90 km is the depth at which pargasitic amphibole ultimately breaks down if the *dehydration solidus* temperatures are not exceeded. This means that in areas where the surface heat flow below the *critical value* (older continental areas, oceanic plates and cratons) there should be a globally occurring horizon of geophysical anomalies at $\sim$90 km. This appears to be in line with global geophysical observations. In Phanerozoic continental areas and oceanic slabs MLD occurring at $\sim$90 km depth may be explained by the break-down of pargasitic amphibole. In these areas sometimes it may be difficult to distinguish the LAB from the MLD. In cratonic areas, however, the distinction between the LAB and MLD is straightforward, and the latter could be due to the break-down of pargasitic amphibole at $\sim$90 km.

Acknowledgements The authors would like to express their honour to Rita Klébesz and an anonymous reviewer for their constructive suggestions which improved our manuscript considerably. Viktor Wesztergom and Eszter Szűcs is kindly acknowledged for his helpful editorial handling. This research was suppoted by a Bolyai Postdoctoral Fellowship to IK.

References

Abt DL, Fischer KM, French SW, Ford HA, Yuan H, Romanowicz B (2010) North American lithospheric discontinuity structure imaged by Ps and Sp receiver functions. J Geophys Res Solid Earth. doi:10.1029/2009JB006914

Artemieva IM (2009) The continental lithosphere: reconciling thermal, seismic, and petrologic data. Lithos 109(1):23–46

Asimow PD, Dixon JE, Langmuir CH (2004) A hydrous melting and fractionation model for mid-ocean ridge basalts: Application to the Mid-Atlantic Ridge near the Azores. Geochem Geophys Geosyst 5(1):2003GC000568. ISSN 1525-2027

Bell DR, Rossman GR (1992) Water in Earth's mantle: the role of nominally anhydrous minerals. Science 255(5050):1391

Carey SW (1958) The tectonic approach to continental drift. In: Carey SW (ed) Continental drift—a symposium. University of Tasmania, Hobart, pp 177–363 (expanding Earth from pp 311–349)

Csontos L, Nagymarosy A, Horváth F, Kovác M (1992) Tertiary evolution of the Intra-Carpathian area: a model. Tectonophysics 208:221–241

Danyushevsky LV, Eggins SM, Fallon TJ, Christie DM (2000) H_2O abundance in depleted to moderately enriched mid-ocean ridge magmas; part I: incompatible behaviour, implications for mantle storage, and origin of regional variations. J Petrol 41(8):1329–1364

Demouchy S, Bolfan-Casanova N (2016) Distribution and transport of hydrogen in the lithospheric mantle: a review. Lithos 240:402–425
Dietz RS (1961) Continent and ocean basin evolution by spreading of the sea floor. Nature 190(4779):854–857
Dixon JE, Leist L, Langmuir C, Schilling JG (2002) Recycled dehydrated lithosphere observed in plume-influenced mid-ocean-ridge basalt. Nature 420(6914):385–389
Dobosi G, Jenner G, Embey-Isztin A, Downes H (2010) Cryptic metasomatism in clino- and orthopyroxene in the upper mantle beneath the Pannonian region. In: Coltorti M (ed) Petrological evolution of the European lithospheric mantle: from Archaean to present day. Geological Society, London, p 337
Dövényi P, Horváth F (1988) Heat flow map of the Pannonian basin and surrounding regions. In: Royden LH, Horváth F (eds) The Pannonian Basin, a study in basin evolution. American Association of Petroleum Geologists Memoir, Tulsa
Embey-Isztin A (1976) Amphibolite/lherzolite composite xenolith from Szigliget, North of the Lake Balaton, Hungary. Earth Planet Sci Lett 31:297–304
Embey-Isztin A, Scharbert HG, Dietrich H, Poultidis H (1989) Petrology and geochemistry of peridotite xenoliths in alkali basalts from the Transdanubian Volcanic Region, West Hungary. J Petrol 30:79–105
Embey-Isztin A, Dobosi G, Altherr R, Meyer HP (2001) Thermal evolution of the lithosphere beneath the western Pannonian Basin: evidence from deep-seated xenoliths. Tectonophysics 331:283–305
Embey-Isztin A, Dobosi G, Bodinier JL, Bosch D, Jenner GA, Pourtales S, Bruguier O (2014) Origin and significance of poikilitic and mosaic peridotite xenoliths in the western Pannonian Basin: geochemical and petrological evidences. Contrib Miner Petrol 168(3):1–16
Faul UH, Jackson I (2005) The seismological signature of temperature and grain size variations in the upper mantle. Earth Planet Sci Lett 234(1):119–134
Fischer M, Ford H, Abt D, Rychert C (2010) The lithosphere-asthenosphere boundary. Annu Rev Earth Planet Sci 38:551–575. doi:10.1146/annurev-earth-040809-152438
Girard J, Chen J, Raterron P, Holyoke CW (2013) Hydrolytic weakening of olivine at mantle pressure: evidence of [100](010) slip system softening from single-crystal deformation experiments. Phys Earth Planet Inter 216:12–20
Green DH (1971) Composition of basaltic magmas as indicators of conditions of origin: application to oceanic volcanism. Philos Trans R Soc Lond 268:707–725
Green DH (1973) Experimental melting studies on a model upper mantle composition at high pressures under water-saturated and water-undersaturated conditions. Earth Planet Sci Lett 19:37–53
Green DH (2015) Experimental petrology of peridotites, including effects of water and carbon on melting in the Earth's upper mantle. Phys Chem Miner 42(2):95–122
Green DH, Falloon TJ (2005) Primary magmas at mid-ocean ridges, "hotspots", and other intraplate settings: constraints on mantle potential temperature. In: Foulger G, Natland J, Presnall D, Anderson D (eds) Plates, Plumes and Paradigms. Geological Society of America Special Paper 388, pp. 217–247
Green DH, Liebermann RC (1976) Phase equilibria and elastic properties of a pyrolite model for the oceanic upper mantle. Tectonophysics 32:61–92
Green DH, Hibberson WO, Kovács I, Rosenthal A (2010) Water and its influence on the lithosphere-asthenosphere boundary. Nature 467(7314):448–451
Green DH, Hibberson WO, Rosenthal A, Kovács I, Yaxley GM, Falloon TJ, Brink F (2014) Experimental study of the influence of water on melting and phase assemblages in the upper mantle. J Petrol 55(10):2067–2096
Griffin WL, Wass SY, Hollis JD (1984) Ultramafic xenoliths from Bullenmerri and Gnotuk maars, Victoria, Australia: petrology of a sub-continental crust-mantle transition. J Petrol 25(1):53–87
Hajnal Z, Reilkoff B, Posgay K, Hegedus E, Takacs E, Asudeh I, Ansorge J, DeIaco R (1996) Crustal-scale extension in the central Pannonian basin. Tectonophysics 264(1):191–204
Hammond WC, Humphreys ED (2000) Upper mantle seismic wave attenuation: effects of realistic partial melt distribution. J Geophys Res Solid Earth 105(B5):10987–10999
Hansen SM, Dueker K, Schmandt B (2015) Thermal classification of lithospheric discontinuities beneath USArray. Earth Planet Sci Lett 431:36–47
Hauri E, Wang J, Dixon JE, King PL, Mandeville C, Newman S (2002) SIMS analysis of volatiles in silicate glasses: 1. Calibration, matrix effects and comparisons with FTIR. Chem Geol 183(1):99–114
Hirschmann MM (2010) Partial melt in the oceanic low velocity zone. Phys Earth Planet Inter 179(1):60–71
Hirth G, Kohlstedt DL (1996) Water in the oceanic upper mantle: implications for rheology, melt extraction and the evolution of the lithosphere. Earth PlanetSci Lett 144(1):93–108
Horváth F (1993) Towards a mechanical model for the formation of the Pannonian basin. Tectonophysics 226(1):333–357

Horváth F, Bada G, Szafián P, Tari G, Ádám A, Cloetingh S (2006) Formation and deformation of the Pannonian Basin: constraints from observational data. Geol Soc Lond Mem 32(1):191–206
Horváth F, Musitz B, Balázs A, Végh A, Uhrin A, Nádor A, Koroknai B, Pap N, Tóth T, Wórum G (2015) Evolution of the Pannonian basin and its geothermal resources. Geothermics 53:328–352
Huismans RS, Podladchikov YY, Cloetingh S (2001) Dynamic modeling of thetransition from passive to active rifting, application to the Pannonian basin. Tectonics 20(6):1021–1039
Jackson I, Faul UH (2010) Grainsize-sensitive viscoelastic relaxation in olivine: to-wards a robust laboratory-based model for seismological application. Phys Earth Planet Inter 183:151–163
Jackson I, Faul U, Skelton R (2014) Elastically accommodated grain-boundary sliding: new insights from experiment and modeling. Phys Earth Planet Inter 228:203–210
Jaupart C, Mareschal JC (1999) The thermal structure and thickness of continental roots. Lithos 48:93–114
Jaupart C, Mareschal JC (2014) Constraints on crustal heat production from heat flow data, treatise on geochemistry, vol 4, 2nd edn. Elsevier, Amsterdam, pp 53–73
Jaupart C, Mareschal JC, Guillou-Frottier L, Davaille A (1998) Heat Flow and thickness of the lithosphere in the canadian Shield. J Geophys Res 103(B7):15269–15286
Karato SI (2014) Does partial melting explain geophysical anomalies? Phys Earth Planet Inter 228:300–306
Karato SI, Olugboji T, Park J (2015) Mechanisms and geologic significance of the mid-lithosphere discontinuity in the continents. Nat Geosci 8(7):509–514
Katz RF, Spiegelman M, Langmuir CH (2003) A new parameterization of hydrous mantle melting. Geochem Geophys Geosyst. doi:10.1029/2002GC000433
Kawakatsu H, Kumar P, Takei Y, Shinohara M, Kanazawa T, Araki E, Suyehiro K (2009) Seismic evidence for sharp lithosphere-asthenosphere boundaries of oceanic plates. Science 324(5926):499–502
Kind R, Yuan X, Kumar P (2012) Seismic receiver functions and the lithosphere–asthenosphere boundary. Tectonophysics 536:25–43
Kiss J, Gúthy T, Zilahi-Sebes L (2016) A Mohorovičić-határfelület magyarországi kutatása–módszerek, mérések, eredmények/Research of the Mohorovičić discontinuity in Hungary (methods, measurements and results). Magyar Geofizika 56(3):152–178
Kohlstedt DL, Keppler H, Rubie DC (1996) Solubility of water in the α, β and γ phases of (Mg, Fe) 2SiO4. Contrib Miner Petrol 123(4):345–357
Konzett J, Armstrong RA, Günther D (2000) Modal metasomatism in the Kaapvaal craton lithosphere: constraints on timing and genesis from U-Pb zircon dating of metasomatized peridotites and MARID-type xenoliths. Contrib Miner Petrol 139(6):704–719
Kovács I, G Falus, Stuart G, Hidas K, Cs Szabó, Flower MFJ, Hegedűs E, Posgay K, Zilahi-Sebess L (2012a) Seismic anisotropy and deformation pat-terns in upper mantle xenoliths from the central Carpathian-Pannonian region: asthenospheric flow as a driving force for Cenozoic extension and extrusion? Tectonophysics 514–517:168–179
Kovács I, Green DH, Rosenthal A, Hermann J, O'Neill HSC, Hibberson WO, Udvardi B (2012b) An experimental study of water in nominally anhydrous minerals in the upper mantle near the water-saturated solidus. J Petrol 53(10):2067–2093
Krézsek C, Bally W (2006) The Transylvanian Basin (Romania) and its relation to the Carpathian fold and thrust belt: insights in gravitational salt tectonics. Mar Pet Geol 23:405–442. doi:10.1016/j.marpetgeo.2006.03.003
Lambert IB, Wyllie PJ (1970) Low-velocity zone of the Earth's mantle: incipient melting caused by water. Science 169(3947):764–766
Lenkey L (1999) Geothermics of the Pannonian basin and its bearing on the tectonics of basin evolution. PhD thesis, Vrije Universiteit, Amsterdam
Lenkey L, Dövényi P, Horváth F, Cloetingh S (2002) Geothermics of the Pannonian basin and its bearing on the neotectonics. In: Cloetingh S, Horváth F, Bada G, Lankreijer A (eds): Neotectonics and surface processes: the Pannonian basin and Alpine/Carpathian system. European Geosciences Union, Stephan Mueller Special Publication Series, vol 3, pp 29–40
Magyar I, Radivojevic D, Sztanó O, Synak R, Ujszászi K, Pócsik M (2012) Progradation of the paleo-Danube shelf margin across the Pannonian Basin during the Late Miocene and Early Pliocene. Glob Planet Change 103:168–173
Mason RG, Raff AD (1961) Magnetic survey off the west coast of the United States between 32°N latitude and 42°N latitude. Bull Geol Soc Am 72(8):1259–1266
McKenzie D (1978) Some remarks on the development of sedimentary basins. Earth Planet Sci Lett 40:25–32
McKenzie D, Bickle MJ (1988) The volume and composition of melt generated by extension of the lithosphere. J Petrol 29:625–697

Michael PJ (1988) The concentration, behavior and storage of H_2O in the suboceanic upper mantle: implications for mantle metasomatism. Geochim Cosmochim Acta 52(2):555–566
Mierdel K, Keppler H, Smyth JR, Falko L (2007) Water solubility in aluminous orthopyroxene and the origin of Earth's asthenosphere. Science 315:364–368. doi:10.1126/science.1135422
Naif S, Key K, Constable S, Evans RL (2013) Melt-rich channel observed at the lithosphere-asthenosphere boundary. Nature 495(7441):356–359
Ni H, Keppler H, Behrens H (2011) Electrical conductivity of hydrous basaltic melts: implications for partial melting in the upper mantle. Contrib Miner Petrol 162(3):637–650
Niida K, Green DH (1999) Stability and chemical composition of pargasitic amphibole in MORB pyrolite under upper mantle conditions. Contrib Miner Petrol 135(1):18–40
Parsons B, Sclater JG (1977) An analysis of the variation of ocean floor bathymetry and heat flow with age. J Geophys Res 82(5):803–827
Peslier AH (2010) A review of water contents of nominally anhydrous natural minerals in the mantles of Earth, Mars and the Moon. J Volcanol Geoth Res 197(1):239–258
Posgay K, Bodoky T, Hegedüs E, Kovácsvölgyi S, Lenkey L, Szafián P, Varga G (1995) Asthenospheric structure beneath a Neogene basin in southeast Hungary. Tectonophysics 252(1):467–484
Rader E, Emry E, Schmerr N, Frost D, Cheng C, Menard J, Geist D (2015) Characterization and petrological constraints of the midlithospheric discontinuity. Geochem Geophys Geosyst 16(10):3484–3504
Royden L, Keen CE (1980) Rifting process and thermal evolution of the continental margin of Eastern Canada determined from subsidence curves. Earth Planet Sci Lett 51:343–361
Royden LH, Horváth F, Nagymarosy A, Stegena L (1983) Evolution of the Pannonian basin system: 2. Subsidence and thermal history. Tectonics 2:91–137
Rychert CA, Shearer PM (2011) Imaging the lithosphere-asthenosphere boundary beneath the Pacific using SS waveform modeling. J Geophys Res Solid Earth. doi:10.1029/2010JB008070
Saal AE, Hauri EH, Langmuir CH, Perfit MR (2002) Vapour undersaturation in primitive mid-ocean-ridge basalt and the volatile content of Earth's upper mantle. Nature 419(6906):451–455
Schmerr N (2012) The Gutenberg discontinuity: melt at the lithosphere-asthenosphere boundary. Science 335(6075):1480–1483
Selway K, Ford H, Kelemen P (2015) The seismic mid-lithosphere discontinuity. Earth Planet Sci Lett 414:45–57
Smyth J, Bell DR, Rossman GR (1991) Incorporation of hydroxyl in upper-mantle clinopyroxenes. Nature 351(6329):732–735
Szabó C, Falus G, Zajacz Z, Kovács I, Bali E (2004) Composition and evolution of lithosphere beneath the Carpathian-Pannonian Region: a review. Tectonophysics 393(1):119–137
Takei Y, Holtzman BK (2009) Viscous constitutive relations of solid-liquid composites in terms of grain boundary contiguity: 1. Grain boundary diffusion control model. J Geophys Res Solid Earth. doi:10.1029/2008JB005850
Tari G, Dövényi P, Dunkl I, Horváth F, Lenkey L, Stefanescu M, Tóth T (1999) Lithospheric structure of the Pannonian basin derived from seismic, gravity and geothermal data. Geol Soc Lond Spec Publ 156(1):215–250
Thybo H (2006) The heterogeneous upper mantle low velocity zone. Tectonophysics 416(1–2):53–79
Thybo H, Perchuc E (1997) The seismic 8 degrees discontinuity and partial melting in continental mantle. Science 275(5306):1626–1629
Wallace M, Green DH (1991) The effect of bulk rock composition on the stability of amphibole in the upper mantle: implications for solidus positions and mantle metasomatism. Mineral Petrol 44(1–2):1–19
Warren JM, Hauri EH (2014) Pyroxenes as tracers of mantle water variations. J Geophys Res Solid Earth 119(3):1851–1881
Wegener A (1912) Die Entstehung der Kontinente. Geologische Rundschau 3(4):276–292. doi:10.1007/BF02202896 **(in German)**
Wilson JT (1963) Hypothesis on the Earth's behaviour. Nature 198(4884):849–865
Xu Z, Gong B, Zhao Z (2016) The water content and hydrogen isotope composition of continental lithospheric mantle and mantle-derived mafic igneous rocks in eastern China. Sci China Earth Sci 59(5):910–926